East European Journal of Physics. 4. 627-634 (2025)
DOI:10.26565/2312-4334-2025-4-66 ISSN 2312-4334

IMPACT OF DONOR-ACCEPTOR POSITIONS TO TUNE EFFICIENT DYE-SENSITIZED SOLAR CELLS: DFT/TD-DFT STUDY

F. Bahrani*, S. Resan, R. Hameed, M. Al-Anber
Molecular Engineering and Computational Modeling Lab, Department of Physics, College of Science, University of Basrah, Basrah, Iraq
**Corresponding Author email: fatimah.bahrani@uobasrah.edu.iq,*
Received August 2, 2025; revised November 10, 2025; accepted November 19, 2025

The anthracene molecule was adopted as a π-conjugation bridge for the D–π–A system with a methyl group CH_3 and a nitro group NO_2 acting as donor and acceptor groups. The influence of the anthracene nature junction with the donor and acceptor sides was evaluated on the performance of a dye-sensitized solar cell (DSSC). The donor and acceptor positions in this study changed around the anthracene. Density functional theory (DFT) has been utilized at the B3LYP theory level. The donor group could bind to anthracene at two specific sites, while the acceptor group could bind to the remaining anthracene sites, excluding the donor group site. The photovoltaic and electronic properties have been investigated. The results showed that the best-performing molecular dyes, $D_{10}A_7$, $D_{10}A_8$, and D_1A_6, are suitable for use as sensitizers due to their energetically favorable photovoltaic parameters, which are attributed to the potential for electron injection and regeneration.
Keywords: *D–π–A; TD-DFT; DSSC; Photovoltaic properties; Anthracene*
PACS: 88.40.hj, 31.15.es**,** 82.47.Jk

INTRODUCTION

Following Grätzel's initial publication, DSSC research garnered significant interest in renewable energy studies because of its affordability, straightforward manufacturing process, and eco-friendly characteristics [1]. Like inorganic dyes, Ruthenium complex-based dyes have good chemical and thermal stability, but are expensive and unavailable [2]**.** Metal complex dye molecules, such as Zn-porphyrin, based on DSSCs have high light-harvesting ability [3]. Metal-free organic dyes have low cost and high absorption coefficients [4]. Although Zn-porphyrin metal complexes based on DSSCs have achieved higher conversion efficiency than metal-free organic dyes, they are costly, highly toxic, and of limited resource [5]. The donor-π-acceptor (D–π–A) moieties are the most prevalent structure in DSSCs due to their light harvesting nature and appropriate modification of the nature of the intramolecular charge transfer [1, 6]. The dye sensitizer absorbs the incident light; therefore, the electron is excited by photoexcitation and moves from the highest occupied molecular orbital (HOMO) to the lowest unoccupied molecular orbital (LUMO) of the dye, as shown in Figure 1 which explain the working principle of DSSCs. The electron is injected into the titanium dioxide (TiO_2) conduction band; therefore, the charge separation occurs at the dye and semiconductor interface through the photo-induced electron injection process. Then, the electron transfers from the TiO_2 to the transparent conducting oxides (TCO) [7]. Thus, the electron reaches from the anode to the cathode and diffuses from the cathode to the electrolyte, so the regeneration of the dye occurs. Based on that, the dye is oxidized to make the DSSC stable and long-lasting [2].

Additionally, the energy level of the redox couple (iodide I^-/triiodide I_3^-) should be higher than the HOMO level of the dye for successful regeneration to occur. The conduction band of the semiconductor metal oxide photo-anode should be below the LUMO level of the dye. The conduction band of TiO_2 should be lower than the LUMO energy level of the dye to allow the electron to be transported to the anode [8]. For potential electron injection and dye regeneration, the HOMO and LUMO levels of the dye should lie with the redox electrolyte (I^-/I_3^-) and the conduction band of TiO_2, respectively [9]. In a molecule, the location of the most energetic electrons is typically considered the HOMO, and it is the most likely location to react with an electrophile. According to a study conducted by Bulat et al. on the HOMO in a molecule, it confidently points to the site of the most energetic electron. It is noted that the HOMO does not consider that the lower energy orbitals in different parts of the molecule may still be occupied by electrons. The lowest values of the average local ionization energy have a considerable influence on the magnitudes and locations of electron density. The HOMO is delocalized and does not point to the lower-lying orbital contributions. Consequently, it is essential to be caution when considering the HOMO as the best energetic electron in a molecule and the most reactive site for the electrophile [10].

Recently, anthracene has been used in DSSCs due to its unique photophysical properties, such as bright blue electroluminescence [11]. When investigating DSSCs, the electron diffusion properties matter, not the luminescent or fluorescent properties. Rapid intramolecular charge transport is crucial in successful electron injection from the anchoring groups of the dye into the conduction band of the semiconductor and successful regeneration back into the dye via the electrolyte. Recombination is crucial in electroluminescence but is a drawback in DSSCs. Anthracene compound is reported in various applications such as light-emitting diodes, thin film transistors, and bulk heterojunction solar cells due to its outstanding optical properties, excellent stability, easy tunability, low cost, and high carrier mobility [12].

Cite as: F. Bahrani, S. Resan, R. Hameed, M. Al-Anber, East Eur. J. Phys. 4, 627 (2025), https://doi.org/10.26565/2312-4334-2025-4-66

The π-conjugated bridge groups help in the electronic transition charge transfer from the ground state to the excited state to enhance the light absorption of DSSCs at a longer wavelength [5, 14, 15], and specify how the π-spacer can facilitate charge transport between different dye fragments. The charge recombination and dye aggregation reduce the efficiency of the metal-free organic dyes [16]. In organic solar cells, fullerenes [15, 17-18] facilitate electron transport, although they have not been studied extensively.

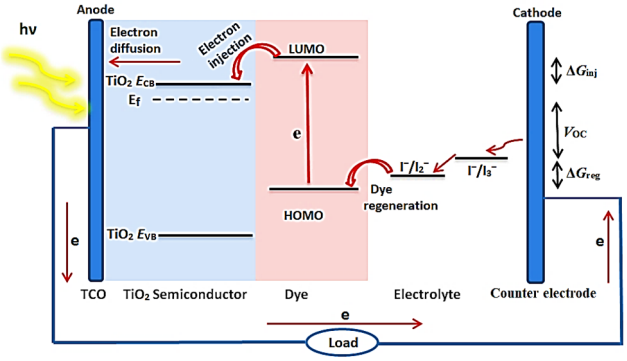

Figure 1. Schematic diagram of the dye-sensitised solar cell (DSSCs) working principle. hν is incident light (photon), e is electron, TCO stands for transparent conducting oxide, TiO_2 is titanium dioxide, E_{CB} is the conduction band edge energy level, E_{VB} is the valence band edge energy level, E_f is the Fermi level, I^-/I_3^- is the iodide/triiodide redox couple, I^-/I_2^- is the iodide/diiodide radical redox pair, HOMO is the highest occupied molecular orbital, LUMO is the lowest unoccupied molecular orbital, ΔG_{inj} is the injection driving force, ΔG_{reg} is the regeneration driving force, and V_{OC} is the open circuit voltage.

Additionally, nanotubes [19, 20] have recently been used in organic solar cells. Nitro group (NO_2) has been employed as a strong electron acceptor group because of its remarkable electron-withdrawing ability and a strong anchoring ability to bond through chemisorption with the semiconductor [21, 22]. In a previous study on benzene and triphenylamine as donors, dimethylanisole as π-conjugated and CN, COOH, and NO_2 as acceptors, Mathiyalagan et al. concluded that triphenylamine and NO_2 have the most potent effect as electron donors and acceptors, respectively, and have perfect optoelectronic properties for use in DSSCs [22]. Methyl group (CH_3) is a substantial electron donor due to its strong electron-donating nature [23]. In a recent work by Bora and Kalita on tetrathiafulvalene as a donor and both cyanoacrylic and carboxylic as acceptors with thiophene as π-conjugation, the dye electron density increased when the CH_3 group and the NO_2 were attached in the donor and acceptor parts, respectively, which maximized the redshift by reducing the energy bandgap [23]. The previous literature generally searched for affective LUMO or HOMO groups to use in D–π–A to get better DSSC efficiency. These studies did not modify the binding sites of these groups; therefore, they did not examine the effect of the choice of binding site to know how the changing sites affected the working cells. In the current research, this has been addressed by studying the D–π–A structure by adding LUMO and HOMO groups and changing their binding sites to find out what effect this change had on the photovoltaic parameters.

This paper used anthracene as a π-spacer between the CH_3 donor and NO_2 acceptor. The position of the donor and acceptor groups around the anthracene was investigated. To evaluate the impact of changing the position of donor and acceptor groups around the π-conjugation on photovoltaic (PV) performance, a molecular orbital with the highest occupied energy E_{HOMO} and a molecular orbital with the lowest unoccupied energy E_{LUMO}, optical bandgap energy (E_g), the maximum absorption wavelengths, oscillator strength (f), light harvesting efficiency (LHE), excited state lifetime (τ), injection driving force (ΔG_{inj}), regeneration driving force (ΔG_{reg}), open circuit voltage (V_{OC}) and fill factor (FF) were illustrated.

COMPUTATIONAL AND THEORETICAL METHODOLOGY

In the D–π–A design, the CH_3, and NO_2 were selected as the donor and acceptor groups, respectively, and they are linked by the anthracene, which acts as a π-conjugation fragment (see Figure 2).

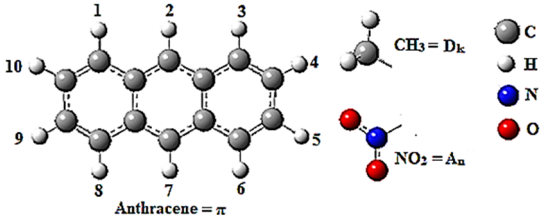

Figure 2. The numbering scheme is used for the variation in functional group positions: D-donor (D_k = CH_3 methyl group) and A-acceptor (A_n = NO_2 nitro group) around the anthracene molecule (π = anthracene); (D_k–π–A_n), where k = 1 or 10, and n = 1, 2,…,10, with k≠n. C, H, N, and O represent carbon, hydrogen, nitrogen, and oxygen, respectively.

According to the numbering D_kA_n = (D_k–π–A_n) in Figure 2, the donor group (D_k) is fixed on anthracene and limited to only two positions, either k = 1 or k = 10, while the acceptor group (A_n) is fixed around the other anthracene positions so that n = 1, 2…10 and k≠n. In this case, when the donor group is fixed on k = 1, the acceptor group will vary on positions

of anthracene (n = 2–10), and when the CH_3 groups are fixed on k = 10, the acceptor groups will vary on positions of anthracene (n = 1–9); therefore, 18 isomers of D_k–π–A_n were obtained. The molecular dye has been studied to explore the influence of changing the position of donor and acceptor groups around the π-conjugated system on the geometries, electronic, and PV properties of the DSSCs.

Complete optimization of these 18 cases was carried out with TD-DFT approaches [24] at B3LYP/6-311G(d,p), where 6-311G(d,p) basis sets for C, H, O, and N, usually approved as a beneficial plan to speculate the molecular structures, based on optimized ground state geometry, were used to evaluate the oscillator strengths and excited state energy calculations. The ground state geometry optimizations for the D_k–π–A_n structure were performed with the Gaussian 09 program package using DFT [25, 26] at the hybrid functional of exchange-correlation B3LYP (Becke three-parameter Lee-Yang-Parr) theory level [26]. Furthermore, all calculations were performed in the gas phase. DSSCs calculations in the real case are more complex than those of the gas phase, where in real DSSCs, dye molecules stick to the TiO_2 surface and are surrounded by a liquid electrolyte. Therefore; the values of ΔG_{inj}, ΔG_{reg}, V_{OC}, and *FF* should be interpreted as qualitative trends. The gas phase does not take these factors into account, and this can affect the dye performance in addition to the overall cell efficiency [27]. However, gas phase calculations are still extremely valuable since they provide initial insights about the electrical and optical properties of the dye [28].

For practical applications, simple chemical methods can be used to bind the methyl (−CH_3) donor group and nitro (−NO_2) acceptor group to the anthracene π -bridge. These groups are added to the anthracene part of the dye to improve DSSCs performance. Common methods such as Friedel-Crafts alkylation or Suzuki coupling can be used to attach the −CH_3 group, whilst the −NO_2 group can be bound through aromatic nitration [28]. Furthermore, a carboxylic acid group is added in the dye to make it stick strongly to the TiO_2 surface [29]. These methods are well established and have been successfully utilized in photovoltaic research [27, 29, 31], our D- π -A dyes are actual and can be surely employed in DSSCs devices.

For PV characterisation, the substantial factor in DSSC is V_{OC} and can be estimated using the commonly used approximately [13]:

$$V_{OC} = E_{\mathrm{LUMO}} - E_{\mathrm{CB}}\,(\mathrm{TiO_2}) \tag{1}$$

where E_{LUMO} is the LUMO energy level of the dye, E_{CB} is the reduction potential of TiO_2 conduction band edge of the semiconductor, with the widely used experimental value of TiO_2 E_{CB} ($E_{\mathrm{CB}} = -4.0$ eV) [33]. All energy values are presented in volts (V), and this expression is intended as a preliminary theoretical estimate. The *FF* have a crucial role in the device efficiency and can be determined as [34]:

$$FF = V_{\mathrm{OC}} - \ln\,(V_{\mathrm{OC}} + 0.72)/(V_{\mathrm{OC}} + 1) \tag{2}$$

LHE, one of the key factors that affects the J_{SC}, is expressed as [35]:

$$LHE = 1 - 10^{-f} \tag{3}$$

where *f* is the oscillator strength of the adsorbed dye molecule related to λ_{max}. The Lambert-Beer law proposes that the *LHE* of a cell relies on the coefficient of dye extinction, the concentration of dye, and the optical path length within the semiconductor film [36]. The lifetime (τ) of the molecular dye can be determined as follows [35]:

$$\tau = 1.499/fE^2 \tag{4}$$

where *E* is the different electron states' excitation energy (cm^{-1}) of the different electronic states. In addition, photovoltaic performance depends on the electron injection rate (ΔG_{inj}) from the dye to the TiO_2 (E_{CB}). Therefore, ΔG_{inj} is beneficial for examining the injection driving force of electrons injected from the dye-excited state E_{LUMO} level to the conduction band of the semiconductor oxide [25]. A negative sign suggests the process of spontaneity [13]. ΔG_{inj} can be determined according to Preat's method [37] as follows [38]:

$$\Delta G_{inj} = E_{\mathrm{dye}*} - E_{CB}(\mathrm{TiO_2}) \tag{5}$$

$E_{\mathrm{dye}*}$ is the oxidation potential energy of the dye molecule in the excited state and can be estimated by:

$$E_{\mathrm{dye}*} = E_{\mathrm{dye}} - E_{0-0} \tag{6}$$

E_{dye} is the oxidation potential of the dye molecule in the ground state (donate $-E_{\mathrm{HOMO}}$), and E_{0-0} is an electronic vertical transition energy corresponding to λ_{max}. ΔG_{reg} is another critical factor that affects the J_{SC} [39]. The significant driving forces of dye regeneration, promote the regeneration efficiency resulting in high J_{SC} [40]. ΔG_{reg} can be calculated as follows [41]:

$$\Delta G_{\mathrm{reg}} = E_{\mathrm{redox}} - E_{\mathrm{dye}} \tag{7}$$

where E_{redox} is the redox potential of the applied electrolyte. Iodide/triiodide (I^-/I_3^-) is typically used as an electrolyte, and the level of couple redox electrolyte (I^-/I_3^-) is about −4.80 eV [25]. Both ΔG_{inj} and ΔG_{reg} represent the change in the free energy in eV for the injection and rejection electrons [13].

RESULTS AND DISCUSSION

Ground state geometry

Knowing the most stable structure for 18 isomers of the D_k–π–A_n is essential to examine the relative energy (ΔE_t). The ground state geometry of D_k–π–A_n was determined using the B3LYP/6-311G(d,p) levels. The differences in ground state energy of the D_k–π–A_n due to the position of donor and acceptor groups around the anthracene are listed in Table 1. The five most stable structures of the anthracene derivatives, with the minimum relative energy (ΔE_t) of 18 isomers, are $D_{10}A_5$, $D_{10}A_4$, D_1A_9, D_1A_4, and D_1A_5, respectively. This indicates that the lowest ground state energy is for $D_{10}A_5$. Generally, a comparison with the previous studies' significant differences [14,18]. Furthermore, no available experimental data are available for comparison.

Frontier molecular orbitals and energy levels

The electronic distribution of frontier orbitals is vital in transferring the effective charge from the donor to the acceptor [5]. The effective charge transfers between the E_{HOMO} and E_{LUMO} levels are substantial for studying the molecular structure of organic PV. The E_{HOMO} levels should be located below the electrolyte I^-/I_3^- (−4.80 eV) [33] to get an efficient dye in DSSCs, and the E_{LUMO} levels should be located above the TiO_2 E_{CB} (−4.0 eV) [33]. Therefore, the electronic and transition properties of the molecule dyes were investigated employing the B3LYP/6-311G(d,p) levels. In our results, all the values of the HOMO level are located below the value of the TiO_2 E_{CB}; therefore, the electron can inject efficiently from the dye to the TiO_2 E_{CB} and the electron can then transfer from the TiO_2 E_{CB} to the TCO and diffuse to the electrolyte. In addition, all the values of the LUMO level are located above the value of the TiO_2 E_{CB}; therefore, the dye can be successfully regenerated back into the dye through electron acceptance from the electrolyte I^-/I_3^-.

The DFT calculated results of E_{HOMO}, E_{LUMO}, and E_g for various positions of the acceptor and donor for D_1A_n and $D_{10}A_n$ are listed in Figure 3. The E_{HOMO} level values of D_k–π–A_n, located below the electrolyte, are in the order D_1A_2, $D_{10}A_1$, $D_{10}A_8$, D_1A_3 and $D_{10}A_3$, respectively. Thus, D_1A_2, $D_{10}A_1$, $D_{10}A_8$, D_1A_3 and $D_{10}A_3$ may enhance the efficient regeneration of electrons back into the dye in DSSCs. In addition, they have the highest ground state energy due to the electrolyte I^-/I_3^-; therefore, they can occur easily and enhance the ΔG_{reg}. E_{HOMO} is often related to the ability [42,43] to donate electrons. Thus, D_1A_2 and $D_{10}A_1$ have the highest electron-donating ability. However, for the E_{LUMO} levels that should be located above the TiO_2 E_{CB}, the highest maximum value in the order of D_k–π–A_n is D_1A_2, $D_{10}A_1$, $D_{10}A_2$, $D_{10}A_7$ and D_1A_7, respectively. The highest value of the E_{LUMO} levels is D_1A_2 despite its high relative stability. Therefore, the effective values of the E_{LUMO} levels that improve the V_{OC} and ΔG_{inj} are for D_1A_2 and D_1A_{10}, respectively, and show the highest electron-accepting ability. Figure 3 illustrates that the energy gap values of D_1A_3, D_1A_6, $D_{10}A_7$, $D_{10}A_6$, and $D_{10}A_3$ are smaller than those of the other dyes (isomers). From previous studies, we expect that the sensitisers with smaller gaps of E_{LUMO}−E_{HOMO} energy show favourable characteristics beneficial to higher *LHE* in the DSSC and facilitate the injection of electrons and the regeneration of dye, which enhances efficiency. Therefore, our designed dyes D_1A_3, D_1A_6, $D_{10}A_7$, $D_{10}A_6$, and $D_{10}A_3$ may have better light harvesting ability than the others [5, 44-46]. Interestingly, we noticed that the decrease in energy gap values is mainly due to decreased LUMO energy levels. This result confirms that the energy levels of the dye sensitisers can be tuned through the donating group's position around the π-conjugated bridge.

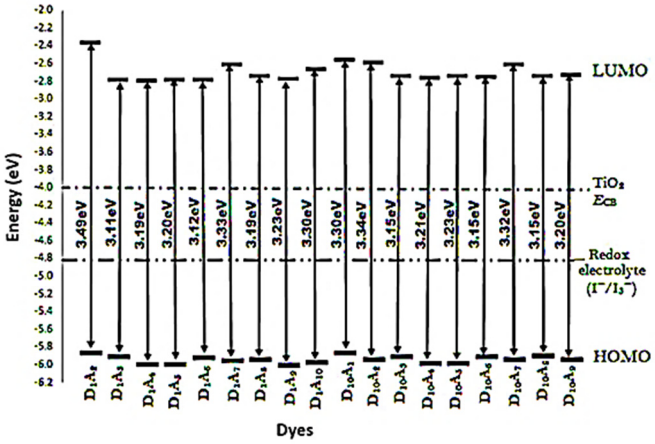

Figure 3. Calculated HOMO- LUMO electronic structures of all studied dyes. TiO_2 E_{CB} represents the conduction band edge of the titanium dioxide (TiO_2); I^-/I_3^- is the redox couple (iodide I^-/triiodide I_3^-), HOMO is the highest occupied molecular orbital, LUMO is the lowest unoccupied molecular orbital

The absorption ability of dye sensitizers plays an essential role in promoting J_{SC}. The solar radiation, including the visible and near-IR range, should be absorbed by a suitable sensitizer in DSSCs [47] as much as possible. Position modifications in the donor-acceptor groups would tune the photo absorption spectra of 18 dye isomers. As Figure 4 shows, the designed dyes D_1A_{10} and $D_{10}A_1$ have the broadest absorption spectra, except for blue shifts. The maximum absorption coefficients of dyes are D_1A_8, D_1A_6, $D_{10}A_5$, D_1A_4, D_1A_9 and $D_{10}A_3$, respectively. The origins of these absorptions are detailed by calculating the singlet electronic transition in the Gaussian 09W program. The maximum absorption peaks of

isomer dyes D_1A_6, $D_{10}A_3$ and D_1A_3 have more redshifts than others. Therefore, we selected D_1A_6, $D_{10}A_3$ and D_1A_3 to design novel dyes further.

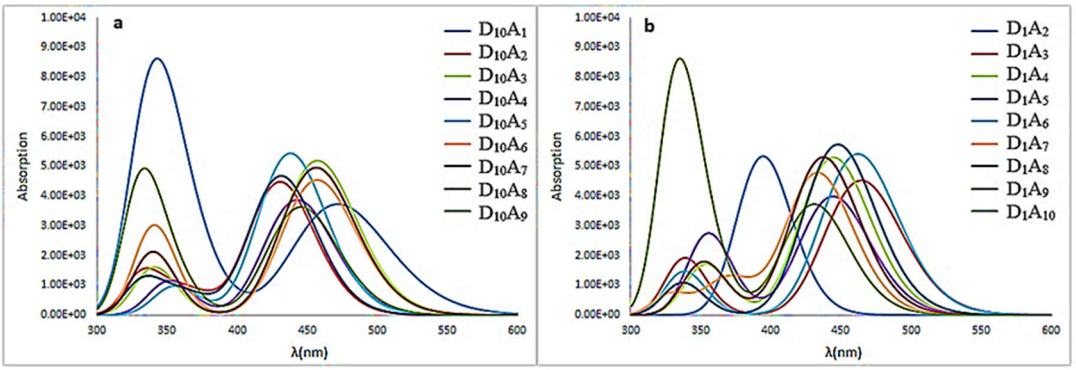

Figure 4. Absorption spectra of 18 dye isomers as a function of wavelength (λ). (a) isomers where the donor group is fixed on the anthracene at site D10, and the acceptor group is bound to the remaining sites. (b) isomers where the donor group is fixed on the anthracene at site D1, and the acceptor group is bound to the remaining sites

Photovoltaic properties

The fundamental factors for characterising an efficient photovoltaic device are V_{OC}, *FF*, *LHE*, τ, ΔG_{inj}, and ΔG_{reg} and are listed in Table 1. These parameters were investigated using TD-DFT theory levels. The impact of the positions of the donor-acceptor groups on the device performance was illustrated.

For increased light-capturing, the *LHE* should be as high as possible to promote the photocurrent and enhance the photovoltaic efficiency. The *LHE* and *f* are directly proportional to each other [13]. The higher *LHE* values in the order are $D_{10}A_7$, D_1A_6, $D_{10}A_5$, $D_{10}A_3$ and $D_{10}A_8$, respectively. Here, $D_{10}A_7$ has the highest *LHE* and can therefore encourage the absorption of the photons and maximise the photocurrent [48]. *LHE* is considered one of the most critical parameters for determining dye efficiency.

Table 1. Calculated relative energy (ΔE_t), oscillator strength (*f*), light harvesting efficiency (*LHE)*, excited state lifetime (τ), injection driving force (ΔG_{inj}), regeneration driving force (ΔG_{reg}), open circuit voltage (V_{OC}), fill factor (*FF*) of dye isomers (D_k–π–A_n)

Position	ΔE_t(eV)	*F*	*LHE*	τ (ns)	ΔG_{inj} (eV)	ΔG_{reg} (eV)	V_{OC} (V)	*FF*
D_1A_2	0.556	0.047	0.103	4.021	−0.955	1.065	1.631	0.890
D_1A_3	0.223	0.062	0.133	2.920	−0.985	1.107	1.212	0.862
D_1A_4	0.047	0.072	0.152	2.838	−0.732	1.192	1.203	0.861
D_1A_5	0.047	0.054	0.116	3.567	−0.821	1.192	1.214	0.862
D_1A_6	**0.228**	**0.075**	**0.159**	**2.485**	**−0.928**	**1.116**	**1.211**	**0.861**
D_1A_7	0.384	0.063	0.134	3.242	−0.774	1.152	1.380	0.875
D_1A_8	0.217	0.065	0.138	2.803	−0.947	1.140	1.255	0.865
D_1A_9	0.037	0.069	0.146	2.959	−0.722	1.207	1.225	0.863
D_1A_{10}	0.240	0.050	0.109	3.848	−0.821	1.175	1.326	0.871
$D_{10}A_1$	0.289	0.052	0.112	4.022	−0.831	1.069	1.436	0.878
$D_{10}A_2$	0.326	0.063	0.134	3.359	−0.739	1.143	1.405	0.876
$D_{10}A_3$	0.183	0.073	0.155	2.628	−0.895	1.107	1.251	0.865
$D_{10}A_4$	0.005	0.055	0.119	3.486	−0.823	1.181	1.237	0.864
$D_{10}A_5$	0.000	0.075	0.158	2.777	−0.711	1.186	1.251	0.865
$D_{10}A_6$	0.184	0.066	0.141	2.770	−0.964	1.109	1.248	0.865
$D_{10}A_7$	**0.329**	**0.079**	**0.167**	**2.463**	**−0.840**	**1.142**	**1.386**	**0.875**
$D_{10}A_8$	**0.185**	**0.073**	**0.155**	**2.540**	**−0.947**	**1.101**	**1.256**	**0.865**
$D_{10}A_9$	0.150	0.052	0.112	3.507	−0.947	1.144	1.263	0.866

A fundamental parameter for DSSC performance is *τ,* which represents the number of diffusing electrons from the excited dye into the TiO_2 E_{CB} semiconductor [39]. In the long lifetime, the charge transfer is facilitated, leading to a potential J_{SC} [49], in contrast, in the short lifetime, the transfer of the charge becomes faster because of electron recombination [39]. *τ* is inversely proportional to *f*. The longer *τ* values for dye isomers order are for $D_{10}A_1$, D_1A_2, D_1A_{10}, D_1A_5, and $D_{10}A_9$, respectively. D_1A_5, $D_{10}A_1$, and D_1A_2 have approximately the most extended value of *τ*; therefore, they can promote the J_{SC} since they have higher generated charge transfer efficiency.

ΔG_{inj} affects the electron injection [39]. The higher absolute value (more negative values) of ΔG_{inj} makes the electron injection more efficient and improves the J_{SC} [39]. E_{dye^*} (E_{LUMO}), which, must be 0.5 eV above TiO_2 E_{CB} to have adequate solar energy converted to current while E_{dye} (E_{HOMO}), which must be 0.2 eV below the redox electrolyte [50-51]. Generally, all the calculated values of ΔG_{inj} have negative sign values; therefore, the electronic injection from the excited state of the dye to the TiO_2 E_{CB} is spontaneous [13]. All values of ΔG_{inj} have less negative potential than the TiO_2 E_{CB} (−4.0eV), which enhances the electron injection from the excited dyes to the TiO_2 E_{CB}. D_1A_3, $D_{10}A_6$, D_1A_2, D_1A_8, $D_{10}A_8$,

and $D_{10}A_9$ exhibit noticeably more negative values and a more stable structure; therefore, they have more efficient electron injection and a higher J_{SC}. J_{SC} is also influenced by the regeneration efficiency of dye (η_{reg}), which is determined by the driving force of regeneration ΔG_{reg}. The regeneration process of dye can significantly influence the efficiency of DSSC. However, higher ΔG_{reg} leads to lower recombination efficiency and represents the increased proportion of absorbed light converted into electrical power [13]. The calculated results of ΔG_{reg} for the dye molecules show that all D_1A_n and $D_{10}A_n$ values have E_{HOMO} levels lower than the electrolyte (−4.80eV), as listed in Table 1 and plotted in Figure 4. The larger ΔG_{reg} values are for D_1A_9, D_1A_4, D_1A_5, $D_{10}A_4$, and $D_{10}A_5$ respectively. D_1A_9 has the greatest ΔG_{reg} values, which enhances the V_{OC} due to the reduction of the recombination reaction, leading to higher photocurrent generation.

In DSSC, the difference in energy between the E_{LUMO} of dye and TiO_2 E_{CB} and the loss in energy via the photo charge generation represents the V_{OC} [52]. The higher E_{LUMO} will produce a higher V_{OC}. The highest V_{OC} values of dyes in the order are for D_1A_2, $D_{10}A_1$, $D_{10}A_2$, $D_{10}A_7$, and D_1A_7, respectively. The highest V_{OC} value for D_1A_2 is equal to 1.631eV. However, *FF* values depend on the V_{OC} [34]. For D_k–π–A_n, the *FF* values are in the order D_1A_2, $D_{10}A_1$, $D_{10}A_2$, $D_{10}A_7$, and D_1A_7, respectively. The range of the *FF* values is between (0.890 to 0.875). The calculated results suggest that D_1A_2, $D_{10}A_1$, $D_{10}A_2$, $D_{10}A_7$, and D_1A_7 have excellent values for V_{OC} and *FF*. Generally, based on our findings, including *LHE*, V_{OC}, *FF*, and ΔG_{in}, we can roughly extrapolate the theoretical current density value and deduce the efficiency's speculative value. Furthermore, according to these results, $D_{10}A_7$, $D_{10}A_8$, and D_1A_6 as molecular dyes could be used as sensitisers since the electron injection process from the excited molecule to TiO_2 E_{CB} is possible.

We evaluate our results by comparing the V_{OC} and *LHE* calculations of our 18 dyes with the theoretical and experimental research. The V_{OC} values of our 18 dyes range from 1.203 to 1.631 V, and *LHE* values range from 0.103 to 0.167, which are consistent with theoretical studies based on DFT [5, 22]. However, for the experimental studies, results of our 18 dyes were compared with those of well-known commercial dyes such as N719 and D149. The V_{OC} values of N719 and D149 [53] range approximately from 0.70 to 0.80 V, and the *LHE* values are about 0.79, as calculated from the absorption spectra of N719 in the 200–500 nm range [54]. Although the calculated *LHE* values for the studied dyes are lower than experimental values for commercial dyes such as N719 and D149, the V_{OC} values are notably higher (1.203-1.631 V) compared to these dyes (0.70–0.80 V), highlighting the potential of our dyes for improved photovoltaic performance. The discrepancy in values is due to difference between theoretical modelling and practical measurement conditions. Overall, the calculated results demonstrate the promising potential of our dyes for improved photovoltaic performance.

CONCLUSIONS

CH_3 and NO_2 were adopted as donor and acceptor groups, respectively, and attached as moieties to the anthracene. Structural, electronic, and photovoltaic parameters affected by the position changing of the donor and acceptor groups around the anthracene were examined theoretically at the B3LYP/6-311G(d,p) level. E_{HOMO}, E_{LUMO}, V_{OC}, *FF*, *LHE*, τ, ΔG_{inj}, and ΔG_{reg} were illustrated to determine their influence on the photovoltaic properties based on the donor and acceptor position around the anthracene. Our results show that all dye molecules in excited states are effective at injecting electrons into the TiO_2 ECB, and that oxidized dyes that lose electrons in the ground state can be restored by accepting electrons from the redox potential. Therefore, the injection and regeneration process is energetically permitted. Notably, the D10A7, D10A8, and D1A6 dyes can be essential for PV parameters, including *LHE*, ΔG_{reg}, V_{OC}, ΔG_{inj}, and *FF*, suggesting that the PV device concept can employ these dye molecules, D10A7, D10A8, and D1A6, as sensitizers.

ORCID

M. Al-Anber, https://orcid.org/0000-0001-9093-6811; **F. Bahrani,** https://orcid.org/0009-0005-4785-0701
S. Resan, https://orcid.org/0000-0003-4214-1314; **R. Hameed,** https://orcid.org/0000-0002-4844-2313

REFERENCES

[1] S. ElKhattabi, A. Fitri, A.T. Benjelloun, *et al*. "Theoretical investigation of electronic, optical and photovoltaic properties of alkylamine-based organic dyes as sensitizers for application in DSSCs," J. Mater. Environ. Sci., **9**(3), 93 (2018). https://doi.org/10.26872/JMES.2018.9.3.93

[2] S.A. Mahadik, H. M. Pathan, and S. Salunke-Gawali, "An Overview of Metal Complexes, Metal-Free and Natural Photosensitizers in Dye-Sensitized Solar Cells,", **24**(0), 1078 (2024) https://doi.org/10.30919/ESEE1078

[3] S.H. Kang, S.Y. Jung, Y.W. Kim, Y.K. Eom, and H.K. Kim, "Exploratory synthesis and photovoltaic performance comparison of D–π–A structured Zn-porphyrins for dye-sensitized solar cells," Dye. Pigment, **149**, 341–347 (2018). https://doi.org/10.1016/J.DYEPIG.2017.10.011

[4] L.C.C. Coetzee, A.S. Adeyinka, and N. Magwa, "A theoretical investigation of decorated novel triazoles as DSSCs in PV devices," J. Mol. Model. **27**(12), 1–16 (2021). https://doi.org/10.1007/S00894-021-04975-Y

[5] A. Slimi, A. Fitri, A.T. Benjelloun, *et al*. "Molecular Design of D-π-A-A Organic Dyes Based on Triphenylamine Derivatives with Various Auxiliary Acceptors for High Performance DSSCs," J. Electron. Mater. **48**(7), 4452–4462 (2019). https://doi.org/10.1007/S11664-019-07228-0

[6] F. Bahrani, R. Hameed, S. Resan, *et al*. "Impact of Torsion Angles to Tune Efficient Dye-Sensitized Solar Cell/Donor-π-Acceptor Model Containing Triphenylamine: DFT/TD-DFT Study," AcPPA, **141**(6), 561–568 (2022). https://doi.org/10.12693/APHYSPOLA.141.561

[7] F.M. Mustafa, A.A.A. Khalek, A.A. Mahboob, and M.K. Abdel-Latif, "Designing Efficient Metal-Free Dye-Sensitized Solar Cells: A Detailed Computational Study," Molecules, **28**(17), 6177 (2023). https://doi.org/10.3390/MOLECULES28176177

[8] A. Azaid, M. Raftani, M. Alaqarbeh, *et al*. "New organic dye-sensitized solar cells based on the D–A–π–A structure for efficient DSSCs: DFT/TD-DFT investigations," RSC Adv. **12**(47), 30626 (2022). https://doi.org/10.1039/D2RA05297K
[9] S. Rahman, A. Haleem, M. Siddiq, *et al*. "Research on dye sensitized solar cells: recent advancement toward the various constituents of dye sensitized solar cells for efficiency enhancement and future prospects," RSC Adv. **13**(28), 19508 (2023). https://doi.org/10.1039/D3RA00903C
[10] F.A. Bulat, J.S. Murray, and P. Politzer, "Identifying the most energetic electrons in a molecule: The highest occupied molecular orbital and the average local ionization energy," Comput. Theor. Chem. **1199**, 113192 (2021). https://doi.org/10.1016/J.COMPTC.2021.113192
[11] B. Li, B. Hou, and G.A.J. Amaratunga, "Indoor photovoltaics, The Next Big Trend in solution-processed solar cells," InfoMat. **3**(5), 445–459 (2021). https://doi.org/10.1002/INF2.12180
[12] M. Harikrishnan, S. Murugesan, and A. Siva, "Novel star-shaped D–π–D–π–D and (D–π)2–D–(π–D)2 anthracene-based hole transporting materials for perovskite solar cells," Nanoscale Adv. **2**(8), 3514–3524 (2020). https://doi.org/10.1039/D0NA00299B
[13] A. Saha, and B. Ganguly, "A DFT study to probe homo-conjugated norbornylogous bridged spacers in dye-sensitized solar cells: An approach to suppressing agglomeration of dye molecules," RSC Adv. **10**(26), 15307–15319 (2020). https://doi.org/10.1039/c9ra10898j
[14] S. Resan, R. Hameed, A. Al-Hilo, and M. Al-Anber, "The Impact of Torsional Angles to Tune the Nonlinear Optical Response of Chalcone Molecule: Quantum Computational Study," Revista Cubana De FiSica, **37**(2), 95–100 (2020).
[15] M. Al-Anber, and S. Resan, "Opto-electronics and nonlinear optical properties of isoindoline-1,3-dione-fullerene20-isoindoline-1,3-dione using density functional theory," Rev. la Fac. Ciencias, **12**(2), 42–63 (2023). https://doi.org/10.15446/REV.FAC.CIENC.V12N2.107224
[16] J. Luo, Z. Wan, C. Jia, Y. Wang, and X. Wu, "A co-sensitized approach to efficiently fill the absorption valley, avoid dye aggregation and reduce the charge recombination," Electrochim. Acta, **215**, 506–514 (2016). https://doi.org/10.1016/J.ELECTACTA.2016.08.072
[17] M. Al-Anber, "Theoretical Semi-empirical Study of the Glycine Molecule Interaction with Fullerene C60," Orbital Electron. J. Chem. **6**(3), 491 (2014). https://doi.org/10.17807/ORBITAL.V6I3.491
[18] M.J. Al-Anber, A.H. Al-Mowali, and A.M. Ali, "Theoretical Semiempirical Study of the Nitrone (Anticancer Drug) Interaction with Fullerene C60 (as Delivery)," Acta Phys. Pol. A, **126**(3), 845–848 (2014). https://doi.org/10.12693/APHYSPOLA.126.845
[19] E. Muchuweni, E.T. Mombeshora, B.S. Martincigh, and V.O. Nyamori, "Recent Applications of Carbon Nanotubes in Organic Solar Cells," Front. Chem. **9**, 733552 (2022). https://doi.org/10.3389/FCHEM.2021.733552
[20] M.J. Al-Anber, "Butyric Acid Interaction with Carbon Nanotubes: Modeling by a Semi-Empirical Approach," Rev. Cuba. Física, **30**(2), 72–76 (2013).
[21] F. Tessore, G. Di Carlo, A. Forni, S. Righetto, F. Limosani, and A.O. Biroli, "Second Order Nonlinear Optical Properties of 4-Styrylpyridines Axially Coordinated to A4 ZnII Porphyrins: A Comparative Experimental and Theoretical Investigation," Inorganics, **8**(8), 45 (2020). https://doi.org/10.3390/INORGANICS8080045
[22] A. Mathiyalagan, K. Manimaran, K. Muthu, and M. Rajakantham, "Density functional theory study on the electronic structures and spectral properties of 3,5-Dimethylanisole dye sensitizer for solar cell applications." Results Chem. **3**, 100164 (2021). https://doi.org/10.1016/J.RECHEM.2021.100164
[23] S.R. Bora, and D.J. Kalita, "Tuning the charge transfer and optoelectronic properties of tetrathiafulvalene based organic dye-sensitized solar cells: a theoretical approach," RSC Adv. **11**(62), 39246–39261 (2021). https://doi.org/10.1039/D1RA05887H
[24] M.E. Casida, C. Jamorski, K.C. Casida, and D.R. Salahub, "Molecular excitation energies to high-lying bound states from time-dependent density-functional response theory: Characterization and correction of the time-dependent local density approximation ionization threshold," J. Chem. Phys. **108**(11), 4439–4449 (1998). https://doi.org/10.1063/1.475855
[25] P.N. Samanta, D. Majumdar, S. Roszak, and J. Leszczynski, "First-Principles Approach for Assessing Cold Electron Injection Efficiency of Dye-Sensitized Solar Cell: Elucidation of Mechanism of Charge Injection and Recombination," J. Phys. Chem. C, **124**(5), 2817–2836 (2020). https://doi.org/10.1021/acs.jpcc.9b10616
[26] B. Miehlich, A. Savin, H. Stoll, and H. Preuss, "Results obtained with the correlation energy density functionals of becke and Lee, Yang and Parr," Chem. Phys. Lett. **157**(3), 200–206 (1989). https://doi.org/10.1016/0009-2614(89)87234-3
[27] E. Mosconi, A. Selloni, and F. De Angelis, "Solvent effects on the adsorption geometry and electronic structure of dye-sensitized TiO_2: A first-principles investigation," J. Phys. Chem. C, **116** (9), 5932–5940 (2012). https://doi.org/10.1021/jp209420h
[28] M.S. Ebied, M. Dongol, M. Ibrahim, M. Nassary, S. Elnobi, and A.A. Abuelwafa, "Effect of carboxylic acid and cyanoacrylic acid as anchoring groups on Coumarin 6 dye for dye-sensitized solar cells: DFT and TD-DFT study," Struct. Chem. **33**(6), 1921-1933 (2022). https://doi.org/10.1007/s11224-022-01957-5
[29] M. Xu, X. Li, Z. Sun, and T. Tu, "Suzuki–Miyaura cross-coupling of bulky anthracenyl carboxylates by using pincer nickel N-heterocyclic carbene complexes: An efficient protocol to access fluorescent anthracene derivatives," Chem. Commun. **49**(98), 11539–11541 (2013). https://doi.org/10.1039/c3cc46663a
[30] G.E. Zervaki, P.A. Angaridis, E.N. Koukaras, G.D. Sharma, and A.G. Coutsolelos, "Dye-sensitized solar cells based on triazine-linked porphyrin dyads containing one or two carboxylic acid anchoring groups," Inorg. Chem. Front. **1**(3), 256–270 (2014). https://doi.org/10.1039/c3qi00095h
[31] A. Siddiqui, N. Islavath, T. Swetha, and S.P. Singh, "D–π–A organic dyes derived from the indacenodithiophene core moiety for efficient dye-sensitized solar cells,"Energy Adv. **2**(7), 1045–1050 (2023). https://doi.org/10.1039/d3ya00060e
[32] B. O'Regan, and M. Grätzel, "A low-cost, high-efficiency solar cell based on dye-sensitized colloidal TiO_2 films," Nature, **353**(6346), 737–740 (1991). https://doi.org/10.1038/353737a0
[33] A.K. Biswas, S. Barik, A. Sen, A. Das, and B. Ganguly, "Design of efficient metal-free organic dyes having an azacyclazine scaffold as the donor fragment for dye-sensitized solar cells," J. Phys. Chem. C, **118**(36), 20763–20771 (2014). https://doi.org/10.1021/jp5049953
[34] B. Kippelen, and J.L. Brédas, "Organic photovoltaics," Energy and Environmental Science, **2**(3), 251–261 (2009). https://doi.org/10.1039/b812502n

[35] A.K. Biswas, A. Das, and B. Ganguly, "Can fused-pyrrole rings act as better π-spacer units than fused-thiophene in dye-sensitized solar cells? A computational study," New J. Chem. **40**(11), 9304–9312 (2016). https://doi.org/10.1039/c6nj02040b
[36] R. Hoffmann, "Interaction of Orbitals through Space and through Bonds," Acc. Chem. Res. **4**(1), 1–9 (1971). https://doi.org/10.1021/ar50037a001
[37] R. Nithya, and K. Senthilkumar, "Theoretical studies on the quinoidal thiophene based dyes for dye sensitized solar cell and NLO applications," Phys. Chem. Chem. Phys. **16**(39), 21496–21505 (2014). https://doi.org/10.1039/c4cp02694b
[38] A. Mahmood, S.U.D. Khan, and U.A. Rana, "Theoretical designing of novel heterocyclic azo dyes for dye sensitized solar cells," J. Comput. Electron. **13**(4), 1033–1041 (2014). https://doi.org/10.1007/s10825-014-0628-2
[39] M.A.M. Rashid, D. Hayati, K. Kwak, and J. Hong, "Theoretical investigation of azobenzene-based photochromic dyes for dye-sensitized solar cells," Nanomaterials, **10**(5), 914 (2020). https://doi.org/10.3390/nano10050914
[40] Z. Yang, C. Liu, C. Shao, C. Lin, and Y. Liu, "First-Principles Screening and Design of Novel Triphenylamine-Based D-A Organic Dyes for Highly Efficient Dye-Sensitized Solar Cells," J. Phys. Chem. C, **119**(38), 21852–21859 (2015). https://doi.org/10.1021/acs.jpcc.5b05745
[41] M. Karuppusamy, V. Surya, K. Choutipalli, D. Vijay, and V. Subramanian, "Rational design of novel N-doped polyaromatic hydrocarbons as donors for the perylene based dye-sensitized solar cells," J. Chem. Sci. (2019), https://doi.org/10.1007/s12039-019-1723-5
[42] H. Assad, R. Ganjoo, and S. Sharma, "A theoretical insight to understand the structures and dynamics of thiazole derivatives," J. Phys. Conf. Ser. **2267**(1), 012063 (2022). https://doi.org/10.1088/1742-6596/2267/1/012063
[43] W. Wang, J. Zhu, Q. Huang, *et al*. "DFT Exploration of Metal Ion-Ligand Binding: Toward Rational Design of Chelating Agent in Semiconductor Manufacturing," Molecules, **29**(2), 203 (2024). https://doi.org/10.3390/MOLECULES29020308
[44] S. El Mzioui, S.M. Bouzzine, I. Sidir, *et al*. "Theoretical investigation on π-spacer effect of the D–π–A organic dyes for dye-sensitized solar cell applications: a DFT and TD-BHandH study," J. Mol. Model. **25**(4), 1–12 (2019). https://doi.org/10.1007/s00894-019-3963-1
[45] A.K. Biswas, A. Das, and B. Ganguly, "The influence of noncovalent interactions in metal-free organic dye molecules to augment the efficiency of dye sensitized solar cells: A computational study," Int. J. Quantum Chem. **117**(18), e25415 (2017). https://doi.org/10.1002/qua.25415
[46] M.I. Abdullah, M.R.S.A. Janjua, A. Mahmood, S. Ali, and M. Ali, "Quantum chemical designing of efficient sensitizers for dye sensitized solar cells," Bull. Korean Chem. Soc. **34**(7), 2093–2098 (2013) https://doi.org/10.5012/BKCS.2013.34.7.2093
[47] M. Prakasam, R. Baskar, K. Gnanamoorthi, and K. Annapoorani, "Triphenylamine Based Organic Dyes with Different Spacers for Dye-Sensitized Solar Cells: A First Principle Study," Int. J. Adv. Sci. Eng. **5**(4), 1118–1124 (2019). https://doi.org/10.29294/IJASE.5.4.2019.1118-1124
[48] Y. Li, Y. Li, P. Song, F. Ma, J. Liang, and M. Sun, "Screening and design of high-performance indoline-based dyes for DSSCs," RSC Adv. **7**(33), 20520–20536 (2017). https://doi.org/10.1039/c6ra28396a
[49] C. Sun, Y. Li, P. Song, and F. Ma, "An experimental and theoretical investigation of the electronic structures and photoelectrical properties of ethyl red and carminic acid for DSSC application," Materials (Basel), **9**(10), 813 (2016). https://doi.org/10.3390/ma9100813
[50] M. Xie, F.-Q. Bai, H.-X. Zhang, and Y.-Q. Zheng, "The influence of inner electric field on the performance of three types of Zn-porphyrin sensitizers in dye sensitized solar cells: A theoretical study," J. Mater. Chem. C, **4**, 10130-10145 (2016). https://doi.org/10.1039/C6TC02457B
[51] M. Xie, L. Hao, R. Jia, J. Wang, and F. Q. Bai, "Theoretical study on the influence of electric field direction on the photovoltaic performance of aryl amine organic dyes for dye-sensitized solar cells," New J. Chem. **43**(2), 651–661 (2019)m https://doi.org/10.1039/C8NJ04360D
[52] M. Hachi, S. El Khattabi, A. Fitri, *et al*. "DFT and TD-DFT studies of the π-bridge influence on the photovoltaic properties of dyes based on thieno[2,3-bindole," J. Mater. Environ. Sci. **9**(4), 1200–1211 (2018).
[53] P.J. Holliman, K.J. Al-Salihi, A. Connell, M.L. Davies, E.W. Jones, and D.A. Worsley, "Development of selective, ultra-fast multiple co-sensitizations to control dye loading in dye-sensitized solar cells," RSC Adv. **4**(5), 2515–2522 (2013). https://doi.org/10.1039/C3RA42131G
[54] E.C. Prima, H.S. Nugroho, Nugraha, G. Refantero, C. Panatarani, and B. Yuliarto, "Performance of the dye-sensitized quasi-solid state solar cell with combined anthocyanin-ruthenium photosensitizer," RSC Adv. **10**(60), 36873–36886 (2020). https://doi.org/10.1039/D0RA06550A

ВПЛИВ ПОЗИЦІЙ ДОНОР-АКЦЕПТОР НА НАЛАШТУВАННЯ ЕФЕКТИВНИХ СОНЯЧНИХ ЕЛЕМЕНТІВ, СЕНСИБІЛІЗОВАНИХ БАРВНИКОМ: DFT/TD-DFT ДОСЛІДЖЕННЯ

Ф. Бахрані, С. Ресан, Р. Хамід, М. Аль-Анбер
Лабораторія молекулярної інженерії та обчислювального моделювання, кафедра фізики, Коледж природничих наук, Університет Басри, Басра, Ірак

Молекулу антрацену було прийнято як π-сполучений місток для системи D–π–A з нітрогрупою CH_3 та нітрогрупою NO2, що діють як донорна та акцепторна групи. Вплив антраценового з'єднання з донорною та акцепторною сторонами було оцінено на продуктивність сонячного елемента, сенсибілізованого барвником (DSSC). Положення донора та акцептора в цьому дослідженні змінювалися навколо антрацену. Теорія функціоналу густини (DFT) була використана на рівні теорії B3LYP. Донорна група могла зв'язуватися з антраценом у двох певних місцях, тоді як акцепторна група могла зв'язуватися з рештою антраценових місць, за винятком донорного місця. Були досліджені фотоелектричні та електронні властивості. Результати показали, що молекулярні барвники з найвищими показниками, $D_{10}A_7$, $D_{10}A_8$ та D_1A_6, придатні для використання як сенсибілізатори завдяки своїм енергетично вигідним фотоелектричним параметрам, які пояснюються потенціалом для інжекції та регенерації електронів.

Ключові слова: *D–π–A; TD-DFT; DSSC; фотоелектричні властивості; антрацен*